Noise and spike-time-dependent plasticity drive self-organized criticality in spiking neural network: towards neuromorphic computing

Narumitsu Ikeda,[1)] Dai Akita,[1)] and Hirokazu Takahashi[1)]

[1]*Graduate School of Information Science and Technology, The University of Tokyo, Tokyo, 113-8656, Japan*

Correspondence should be addressed to Hirokazu Takahashi (takahashi@i.u-tokyo.ac.jp)
The University of Tokyo, 7-3-1 Hongo, Bunkyo-ku, Tokyo, 11308656, Japan

Abstract

Self-organized criticality (SoC) may optimize information transmission, encoding, and storage in the brain. Therefore, the underlying mechanism of the SoC provides significant insights for large-scale neuromorphic computing. We hypothesized that noise and stochastic spiking plays an essential role in SoC development in spiking neural networks (SNN). We demonstrated that under appropriate noise levels and spike-time-dependent plasticity (STDP) parameters, an SNN evolves a SoC-like state characterized by a power-law distribution of neuronal avalanche size in a self-organized manner. Consistent with the physiological findings, the development of SNN was characterized by a transition from a subcritical state to a supercritical state and then to a critical state. Excitatory STDP with an asymmetric time window dominated the early phase of development; however, it destabilized the network and transitioned to the supercritical state. Synchronized bursts in the supercritical state enable inhibitory STDP with a symmetric time window, induce the development of inhibitory synapses, and stabilize the network towards the critical state. This sequence of transitions was observed when the appropriate noise level and STDP parameters were set to the initial conditions. Our results suggest that noise or stochastic spiking plays an essential role in SoC development and self-optimizes SNN for computation. Such neural mechanisms of noise harnessing would offer insights into the development of energy-efficient neuromorphic computing.

Main Text

Self-organized criticality (SoC) underlies the complexity of natural large-scale dynamic systems, which are characterized by temporal or spatial self-similarity with power-law correlations (1, 2). The brain also exhibits SoC-like dynamics or the "neuronal avalanche" characterized as power-law distribution of activation size (3-6), which possibly optimizes computing performance, such as information transmission (3, 7), encoding, and storage (8-11). Furthermore, under a particular

condition, the SoC is associated with the "edge of chaos," another critical state of dynamical systems that optimizes the performance of reservoir computing with recurrent neural networks (12-17). Therefore, the underlying mechanism of the SoC may provide significant insights into the self-optimization of large-scale neuromorphic computing (18-20).

The seminal model of "sand-pile automata" demonstrated that dissipative dynamical systems with both temporal and spatial degrees of freedom can evolve towards an SoC state (1). More recently, the neural mechanisms of SoC development have been discussed in simulation models with the activity-dependent outgrowth of neuronal processes (21-23), spiking neural networks (SNNs) with short-term plasticity (STP), and long-term spike-time-dependent plasticity (STDP) (24, 25). However, these models do not always fully explain the physiological findings of neural development. First, the SoC emerges through a two-step transition of developmental phases in dissociate cultures of neurons (22, 26-32): Before the growth of neuronal processes, i.e., without any synaptic connection, neuronal activities in culture initially exhibited an asynchronized state, or "subcritical state," with an exponential distribution of neural avalanche; culture at the growth phase was then characterized as a regularly synchronized state, or "supercritical state," with a bimodal distribution; matured culture finally reached a "critical state" with a power-law distribution. Second, the development of a critical state in neuronal cultures is associated with a balance between excitation and inhibition (E/I balance) (9, 22, 28). Third, a stable network structure with a core topography and rich club organization emerged during development (33-35). Therefore, a better model of the SoC in a neural network is expected to explain these experimental findings.

We hypothesize that a simple SNN evolves the SoC in a physiologically plausible manner through spontaneous activity with an appropriate level of noise and STDP parameters. Starting from a neuron population with no synaptic connections, we simulated how network development depends on the noise level and STDP. We predict that SNN development under appropriate parameters corroborates the following physiological findings: (i) the initial network would exhibit an asynchronized, subcritical state; (ii) excitatory STDP with a temporally asymmetric time window would gradually develop a rich club topography, produce synchronized bursts, and transition to the supercritical state (36); (iii) the bursts would then enable inhibitory STDP with a temporally symmetric time window, stabilize the network through an E/I balance, and develop a critical state (37).

Based on (24), we developed SNNs with escape noise (38), in which each neuron spontaneously discharges in a Poisson process. The model and parameters are described in detail in the

Supplementary Information. In our simulation, which mimicked the development of dissociate culture of neurons, the strength of the synapses between neurons was initially set to zero and developed through spontaneous activity according to the STDP, as shown in Fig. 1. The main parameters β_E and β_I determined the ratio of long-term depression (LTP) to potentiation (LTD) in excitatory and inhibitory synapses, respectively; for example, β_E =1.2 implied that LTD was stronger than LTP in excitatory synapses. The level of escape noise, that is, the firing rate of each neuron around the resting membrane potential, also served as another main parameter.

Figure 2a shows representative raster plots at 0, 6, and 72 h after the initialization. Initially, each neuron had a firing rate of 0.4 Hz without any synaptic input, and STDP parameters were set at β_E =1.00 and β_I =1.15. Throughout development, SNN exhibited three distinct states characterized by neuronal avalanche size distribution (Fig. 2b): the subcritical state (exponential distribution) at 0 h, supercritical state (bimodal distribution) at 6 h, and critical state (power-law distribution) at 72 h. Additional tests also supported the scale-free behavior of neuronal avalanche in the critical state(22): (i) the power-law distribution of avalanche sizes was robustly observed with less neurons and different time bins, suggesting that the neuronal avalanche was both spatially and temporally scale-free (Supplementary Fig. S1a and b); (ii) the inter-avalanche intervals exhibited the scale-free behaviors (Supplementary Fig. S1c); and (iii) The Fano factor, $F(T)$, i.e., the number of spikes within a time window t to $t + T$, was characterized as a power-law form of T^{α} (39) with α ranging between 0.62 and 0.83 (median 0.73), which is consistent with physiological data (Supplementary Fig. S1d). This state transition was associated with synaptic development (Fig. 2c). In the subcritical state, excitatory synapses gradually strengthened whereas inhibitory synapse did not develop, i.e., $W_{II} \approx 0$ before 6h; in the supercritical state, inhibitory synapses rapidly grew; in the critical state, excitatory-to-excitatory synapses (w_{EE}) and inhibitory-to-excitatory synapses (w_{IE}) polarized into strong and weak weights, suggesting the development of core topology (33). The average of network parameters across networks proved that each SNN exhibited a similar pattern of development (Fig. 2c, right column) and that this pattern was consistent with dissociate culture of neurons (22, 26-32): LLR (log-likelihood ratio (3, 26)) indicated the avalanche size characteristics transitioned from exponential to power-law distribution; D (Bimodality index (26)) indicated bimodal distribution at the growth stage, that is, 6 h; ΔCr (Criticality index, modified from Δp in (22) as defined in supplementary information) indicated that the criticality was gradually achieved; BI (burstiness index (40)) indicated that the synchronized bursts were observed most distinctly at the growth stage and gradually reached the plateau at a certain level at the maturation. Development of the critical state was also associated with the growth of firing rate in the network (Fig. 2d) and the EI balance in each neuron in the SNN (Fig. 2e). The critical state was maintained after the STDP was disabled (Supplementary

Fig. S2), indicating that the STDP plays a crucial role in the development, but not in the maintenance of the critical state. Inappropriate STDP parameters lead to either subcritical or supercritical states (Supplementary Fig. S3).

After sufficient development of 72 h, where the network parameters were stable for at least 24 h, SNN reached either a supercritical, critical, or subcritical state, depending on β_E and β_I (Fig. 3a). Some SNNs developed a critical state with small β_I (<1), where inhibitory synapses were strengthened without bursts, but these SNNs did not exhibit two-step transition of developmental phases (Supplementary Fig. S4; $\beta_E = 1.10$, $\beta_I = 0.80$). Our parameter search indicated that SNN was stabilized at a supercritical state with β_E and β_I around 1 (LTP $\approx$ LTD), while at a subcritical state with large β_E and β_I (LTD > LTP) (Fig. 3b). The critical state region was found in the β_E-β_I plane even when the STDP time scale was doubled or halved (Supplementary Fig. S5). Thus, the critical state in the SNN was achieved using appropriate STDP parameters.

The noise level also affects the SNN activity and state. Irrespective of the STDP parameters, the firing rates per neuron in the developed SNN were higher than those in the initial condition, that is, the noise level, and increased nonlinearly with the noise level (Fig. 4a). A certain noise level or higher destabilizes the SNN with aberrant bursts and firing rates as high as 100 Hz. Small β_E (<1), where LTP > LTD, also destabilized the SNN (Fig. 4b). Conversely, a low noise level was more likely to develop subcritical SNN ($\Delta Cr<0$) (Fig. 4c). Our parameter search indicated that the critical SNN ($\Delta Cr\approx0$) was developed with appropriate noise and STDP parameters.

The noise level and STDP parameters also affected the synaptic stability in the SNN. Figure 5a showed the proportion of synapses that maintained synaptic strength at 0.5 or larger between 60 h to 72 h in simulation time. The proportion decayed with the noise level in the EE, EI, IE, and II synapses, indicating that the core topology with stable synapses could not be maintained at a noise level of 0.4 Hz or higher. The core topology was disrupted by inappropriate STDP parameters with large β_E and β_I (LTD > LTP) (Fig. 5b). Thus, noise and STDP in SNN are essential for SoC development; however, excessively high noise and inappropriate STDP parameters break the core topology.

We demonstrated that under an appropriate noise level and STDP parameters, the SNN evolves into a critical state characterized by a power-law distribution of the neuronal avalanche size in a self-organized manner. Consistent with physiological findings, the development of SNN is characterized as a transition from a subcritical state to a supercritical state, and then to a critical state (22, 26-32). Excitatory STDP with an asymmetric time window played a crucial role in

dichotomization of strong vs. weak synapses (Fig. 2c) and high vs. low firing-rate excitatory neurons (Fig. 2d), and thereby in establishing a rich club topography in the early phase of development (33-35), but in turn, destabilized the network and transitioned to the supercritical state. Because inhibitory STDP with a symmetric time window was more effective with synchronized bursts in the supercritical state than in the asynchronous subcritical state, inhibitory synapses developed later than excitatory synapses in the supercritical state, where the network was stabilized and an E/I balance was achieved (9, 22, 28). This sequence of transitions was observed when the appropriate noise level and STDP parameters were set to the initial conditions.

Some models to achieve SoC in neural networks only consider excitatory synaptic plasticity and hypothesize that the homeostatic property of the global activity level stabilizes the network (21, 23). As each neuron has no access to the global activity level, inhibition is a more biologically plausible mechanism than a homeostatic activity to stabilize the network (22, 24, 25). SoC development was previously demonstrated in an SNN model with excitatory and inhibitory STDP (22), whose parameters depend on the developmental phases, that is, subcritical, critical, and supercritical states. In this study, we further demonstrate that these states transition in a self-organized manner with fixed parameters throughout the development.

Inhibition stabilization offers additional advantages in cortical computing, such as efficient coding and nonlinear computation (41, 42). The E/I balance is an emergent property of large-scale neural networks with excitatory and inhibitory synapses and underlies a rich repertoire of spatiotemporal patterns (43). Thus, inhibitory STDP can play a crucial role in modulating E/I balance and maintaining network dynamics (37, 44 , 45). For example, network dynamics maintained at the edge of chaos optimize reservoir computing using recurrent neural networks (12-17). Although the computational performance depends on how tight the E/I balance is achieved in the network, our results suggest that the noise level and STDP parameters in the network reflect an optimal tradeoff between the computational performance in a given task and the maintenance cost of a highly structured network (42).

While some synaptic weights fluctuated over time, such as the spine size (46, 47), a significant portion of the weights remained stable over time in our SNN. These stable synaptic connections were consistent with the physiological experiments. For example, a core topology with stable synaptic connections was found in a dissociated culture of neurons (33); a significant proportion (50% or more) of spines in the neocortex are long lasting, with a lifetime as long as a month (48, 49). Our results suggest that the noise level and STDP parameters are critical for synapse stability.

We have settled the bound on synaptic weights, which is widely accepted and biologically plausible because spatial limitation is imposed on spine size development. However, the bound did not vary among synapses. Such uniform thresholding might cause problematic effects on avalanche development (50). Future works are still needed to address how the bound of synaptic weights affect neuronal avalanche development.

Because noise that disturbs signals is problematic for information processing, a computational chip is designed to ensure a sufficient signal-to-noise ratio, which in turn becomes more energy-consuming than the brain (18-20). As noise is inevitable in biochemical systems, noise-tolerant computational mechanisms must be implemented in the brain (51). Furthermore, several studies have suggested that the brain and SNN harness noise for information processing (52), such as stochastic resonance (53), simulated annealing (54), and noise-induced chaos-order transitions (55, 56). Our results also suggest that noise or stochastic spiking plays an essential role in SoC development and self-optimizes SNN for computation. In particular, such self-optimization would boost information processing capacity of reservoir computing with SNN (57). These neural mechanisms of noise harnessing would offer insights into the development of energy-efficient neuromorphic computing.

Figures

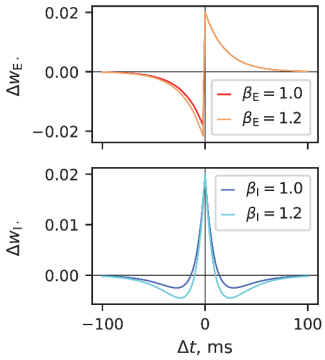

Figure 1. Spike-time-dependent plasticity (STDP) parameters. The ratio of long-term depression (LTD) to potentiation (LTP) strength was determined by β_E and β_I in excitatory and inhibitory synapses, respectively.

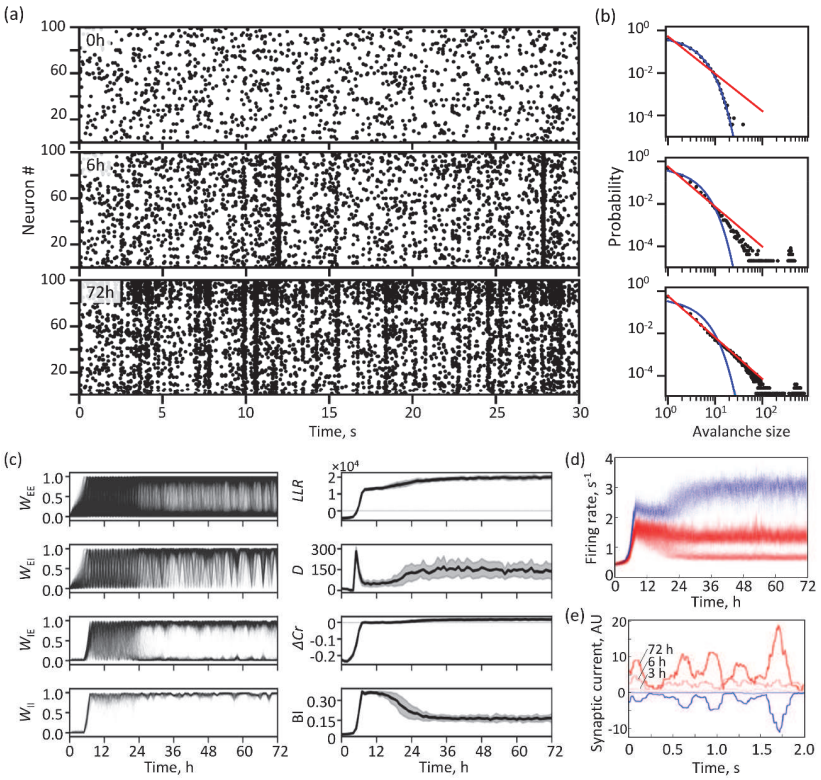

Figure 2. Development of SNN to the critical state. (a) Representative raster plots of spontaneous activities at 0 (top), 6 (middle), and 72 h (bottom) after the initialization. (b) Neuronal avalanche distributions in (a). The maximum likelihood estimations of the exponential and power-law distributions were shown in blue and red, respectively. (c) Time courses of network characteristics. (left) Synaptic weights during development in (a). (right) Population activity characteristics: LLR, log-likelihood ratio, i.e., power-law distribution index; D, bimodal distribution index; ΔCr, criticality index; and BI, burstiness index. The mean and standard deviations are provided (bold lines and shaded areas) for 30 neural networks with different random seeds. (d) Time course of firing rate. Each trace indicates an individual neuron: red, excitatory neurons; blue, inhibitory neurons. (e) Excitatory-to-inhibitory (EI) balance in the critical state. The moving average of excitatory current $I_{exc} = (E_{exc} - v)g_{exc}$ (red) and inhibitory current $I_{inh} = (E_{inh} - v)g_{inh}$ (blue) with a 150 ms time window for a spontaneously spiking neuron at the development stage of 3 (light), 6, and 72 h (dark). The excitatory and inhibitory currents were correlated at the

developed state.

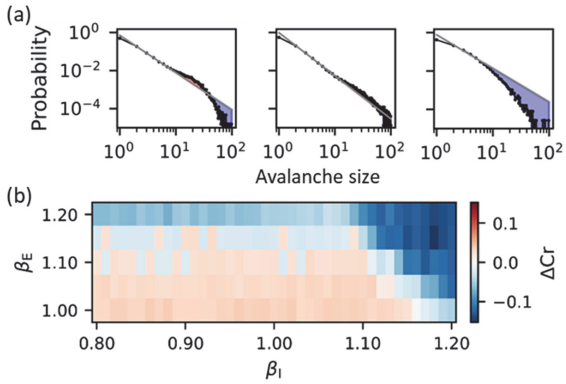

Figure 3. STDP parameter search for SNN development. (a) Characterization of neuronal avalanches. Representative avalanche distributions of supercritical (left), critical (middle), and subcritical states (right) are shown. The grey lines are the fitted lines to derive ΔCr. (b) ΔCr as a function of STDP parameters of β_E and β_I.

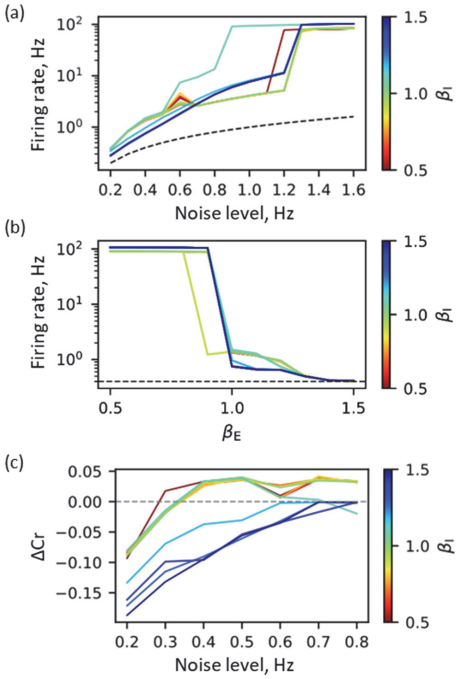

Figure 4. Noise-level-dependent SNN development. (a) Firing rate as a function of noise level. β_E was fixed at 1.0. β_I was manipulated as shown in color. (b) Firing rate as a function of β_E. Noise level was fixed at 0.4 Hz. (c) ΔCr as a function of noise level.

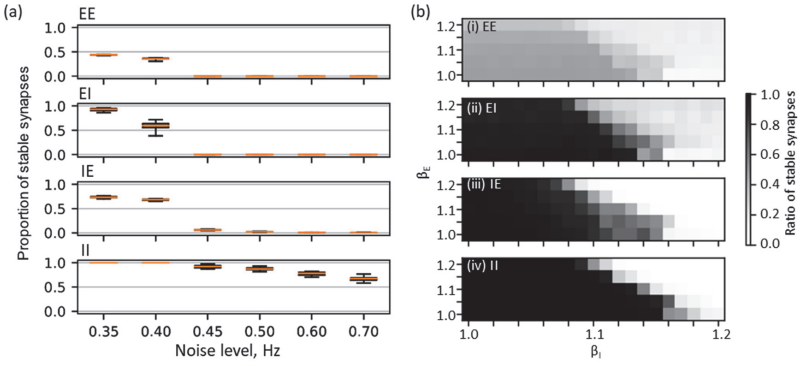

Figure 5. Stability of synaptic weights. (a) Proportions of weights maintained at 0.5 or larger from the developmental time between 60 and 72 h are shown for excitatory-to-excitatory (EE), excitatory-to-inhibitory (EI), inhibitory-to-excitatory (IE), and inhibitory-to-inhibitory (II) synapses. STDP parameters were set at β_E =1.00 and β_I =1.15. (b) STDP-parameter vs. synaptic stability. In the β_E-β_I plane, proportions of weights maintained at 0.5 or larger from the developmental time between 60 and 72 h are shown for (i) excitatory-to-excitatory (EE), (ii) excitatory-to-inhibitory (EI), (iii) inhibitory-to-excitatory (IE), and (iv) inhibitory-to-inhibitory (II) synapses. The noise level was set at 0.4 Hz.

Supplementary Materials

Supplementary Figures S1 to S5
Methods

Acknowledgment:

This work was partially supported by JSPS KAKENHI (20H04252), AMED (JP21dm0307009), NEDO (18101806-0), JST (JPMJMS2296), and the Asahi Glass Foundation.

Conflict of interest

The authors have no conflicts to disclose.

Author Contributions

NI: formal analysis, investigation, methodology, software, visualization, writing-original draft
DA: formal analysis, investigation, validation, visualization, writing-review & editing
HT: conceptualization, funding acquisition, project administration, supervision, writing-review & editing

Data availability statement:

The data supporting the findings of this study are available from the corresponding author upon reasonable request.

References

1. P. Bak, C. Tang, K. Wiesenfeld, Self-organized criticality: An explanation of the 1/f noise. *Physical review letters* **59**, 381-384 (1987).
2. M. A. Muñoz, Colloquium: Criticality and dynamical scaling in living systems. *Rev Mod Phys* **90**, 031001 (2018).
3. J. Beggs, D. Plenz, Neuronal avalanches in neocortical circuits. *J Neurosci* **23**, 11167-

11177 (2003).

4. D. Plenz, T. Thiagarajan, The organizing principles of neuronal avalanches, cell assemblies in the cortex. *Trends Neurosci* **30**, 101-110 (2007).
5. D. Plenz, T. L. Ribeiro, S. R. Miller *et al.*, Self-Organized Criticality in the Brain. *Frontiers in Physics* **9** (2021).
6. Z. Bowen, D. E. Winkowski, S. Seshadri, D. Plenz, P. O. Kanold, Neuronal Avalanches in Input and Associative Layers of Auditory Cortex. *Frontiers in systems neuroscience* **13** (2019).
7. W. L. Shew, H. Yang, S. Yu, R. Roy, D. Plenz, Information capacity and transmission are maximized in balanced cortical networks with neuronal avalanches. *J Neurosci* **31**, 55-63 (2011).
8. J. M. Beggs, D. Plenz, Neuronal avalanches are diverse and precise activity patterns that are stable for many hours in cortical slice cultures. *J Neurosci* **24**, 5216-5229 (2004).
9. W. L. Shew, H. Yang, T. Petermann, R. Roy, D. Plenz, Neuronal avalanches imply maximum dynamic range in cortical networks at criticality. *J Neurosci* **29**, 15595-15600 (2009).
10. C. Haldeman, J. M. Beggs, Critical branching captures activity in living neural networks and maximizes the number of metastable states. *Physical review letters* **94** (2005).
11. R. Stoop, F. Gomez, Auditory Power-Law Activation Avalanches Exhibit a Fundamental Computational Ground State. *Physical review letters* **117**, 038102 (2016).
12. Ł. Kuśmierz, S. Ogawa, T. Toyoizumi, Edge of Chaos and Avalanches in Neural Networks with Heavy-Tailed Synaptic Weight Distribution. *Physical review letters* **125**, 028101 (2020).
13. H. Sompolinsky, A. Crisanti, H. J. Sommers, Chaos in Random Neural Networks. *Physical review letters* **61**, 259-262 (1988).
14. N. Bertschinger, T. Natschlager, Real-time computation at the edge of chaos in recurrent neural networks. *Neural Comput* **16**, 1413-1436 (2004).
15. D. Verstraeten, B. Schrauwen, M. D'Haene, D. Stroobandt, An experimental unification of reservoir computing methods. *Neural Networks* **20**, 391-403 (2007).
16. D. Sussillo, L. F. Abbott, Generating coherent patterns of activity from chaotic neural networks. *Neuron* **63**, 544-557 (2009).
17. R. Laje, D. V. Buonomano, Robust timing and motor patterns by taming chaos in recurrent neural networks. *Nat Neurosci* **16**, 925-933 (2013).
18. A. Mehonic, A. J. Kenyon, Brain-inspired computing needs a master plan. *Nature* **604**, 255-260 (2022).
19. K. Roy, A. Jaiswal, P. Panda, Towards spike-based machine intelligence with

neuromorphic computing. *Nature* **575**, 607-617 (2019).

20. S. Furber, Large-scale neuromorphic computing systems. *J Neural Eng* **13**, 051001 (2016).
21. L. F. Abbott, R. Rohrkemper, "A simple growth model constructs critical avalanche networks" in Progress in Brain Research, P. Cisek, T. Drew, J. F. Kalaska, Eds. (Elsevier, 2007), vol. 165, pp. 13-19.
22. C. Tetzlaff, S. Okujeni, U. Egert, F. Wörgötter, M. Butz, Self-Organized Criticality in Developing Neuronal Networks. *Plos Comput Biol* **6**, e1001013 (2010).
23. F. Y. K. Kossio, S. Goedeke, B. van den Akker, B. Ibarz, R. M. Memmesheimer, Growing Critical: Self-Organized Criticality in a Developing Neural System. *Physical review letters* **121** (2018).
24. N. Stepp, D. Plenz, N. Srinivasa, Synaptic Plasticity Enables Adaptive Self-Tuning Critical Networks. *Plos Comput Biol* **11**, e1004043 (2015).
25. B. Del Papa, V. Priesemann, J. Triesch, Criticality meets learning: Criticality signatures in a self-organizing recurrent neural network. *Plos One* **12**, e0178683 (2017).
26. Y. Yada, T. Mita, A. Sanada *et al.*, Development of neural population activity toward self-organized criticality. *Neuroscience* **343**, 55-65 (2017).
27. J. J. Sun, W. Kilb, H. J. Luhmann, Self-organization of repetitive spike patterns in developing neuronal networks in vitro. *Eur J Neurosci* **32**, 1289-1299 (2010).
28. V. Pasquale, P. Massobrio, L. L. Bologna, M. Chiappalonea, S. Martinoia, Self-organization and neuronal avalanches in networks of dissociated cortical neurons. *Neuroscience* **153**, 1354-1369 (2008).
29. D. A. Wagenaar, J. Pine, S. M. Potter, An extremely rich repertoire of bursting patterns during the development of cortical cultures. *Bmc Neurosci* **7** (2006).
30. M. Chiappalone, M. Bove, A. Vato, M. Tedesco, S. Martinoia, Dissociated cortical networks show spontaneously correlated activity patterns during in vitro development. *Brain Res* **1093**, 41-53 (2006).
31. P. van, J, P. Wolters, M. Corner, W. Rutten, G. Ramakers, Long-term characterization of firing dynamics of spontaneous bursts in cultured neural networks. *IEEE transactions on bio-medical engineering* **51**, 2051-2062 (2004).
32. H. Kamioka, E. Maeda, Y. Jimbo, H. P. C. Robinson, A. Kawana, Spontaneous periodic synchronized bursting during formation of mature patterns of connections in cortical cultures. *Neurosci Lett* **206**, 109-112 (1996).
33. J. Van Pelt, M. A. Corner, P. S. Wolters, W. L. Rutten, G. J. Ramakers, Longterm stability and developmental changes in spontaneous network burst firing patterns in dissociated rat cerebral cortex cell cultures on multielectrode arrays. *Neurosci Lett* **361**, 86-89 (2004).

34. M. S. Schroeter, P. Charlesworth, M. G. Kitzbichler, O. Paulsen, E. T. Bullmore, Emergence of rich-club topology and coordinated dynamics in development of hippocampal functional networks in vitro. *J Neurosci* **35**, 5459-5470 (2015).
35. S. Nigam, M. Shimono, S. Ito *et al.*, Rich-Club Organization in Effective Connectivity among Cortical Neurons. *J Neurosci* **36**, 670-684 (2016).
36. N. Caporale, Y. Dan, Spike Timing–Dependent Plasticity: A Hebbian Learning Rule. *Annual Review of Neuroscience* **31**, 25-46 (2008).
37. T. P. Vogels, H. Sprekeler, F. Zenke, C. Clopath, W. Gerstner, Inhibitory plasticity balances excitation and inhibition in sensory pathways and memory networks. *Science* **334**, 1569-1573 (2011).
38. H. E. Plesser, W. Gerstner, Noise in Integrate-and-Fire Neurons: From Stochastic Input to Escape Rates. *Neural Comput* **12**, 367-384 (2000).
39. S. B. Lowen, T. Ozaki, E. Kaplan, B. E. A. Saleh, M. C. Teich, Fractal Features of Dark, Maintained, and Driven Neural Discharges in the Cat Visual System. *Methods* **24**, 377-394 (2001).
40. D. A. Wagenaar, R. Madhavan, J. Pine, S. M. Potter, Controlling bursting in cortical cultures with closed-loop multi-electrode stimulation. *J Neurosci* **25**, 680-688 (2005).
41. S. Sadeh, C. Clopath, Inhibitory stabilization and cortical computation. *Nat Rev Neurosci* **22**, 21-37 (2021).
42. S. Denève, C. K. Machens, Efficient codes and balanced networks. *Nat Neurosci* **19**, 375-382 (2016).
43. C. V. Vreeswijk, H. Sompolinsky, Chaos in Neuronal Networks with Balanced Excitatory and Inhibitory Activity. *Science* **274**, 1724-1726 (1996).
44. R. C. Froemke, Plasticity of Cortical Excitatory-Inhibitory Balance. *Annual Review of Neuroscience, Vol 38* **38**, 195-219 (2015).
45. G. Hennequin, E. J. Agnes, T. P. Vogels, Inhibitory Plasticity: Balance, Control, and Codependence. *Annual Review of Neuroscience* **40**, 557-579 (2017).
46. Y. Loewenstein, A. Kuras, S. Rumpel, Multiplicative Dynamics Underlie the Emergence of the Log-Normal Distribution of Spine Sizes in the Neocortex In Vivo. *The Journal of Neuroscience* **31**, 9481-9488 (2011).
47. N. Yasumatsu, M. Matsuzaki, T. Miyazaki, J. Noguchi, H. Kasai, Principles of Long-Term Dynamics of Dendritic Spines. *The Journal of Neuroscience* **28**, 13592-13608 (2008).
48. A. Attardo, J. E. Fitzgerald, M. J. Schnitzer, Impermanence of dendritic spines in live adult CA1 hippocampus. *Nature* **523**, 592-596 (2015).
49. J. T. Trachtenberg, B. E. Chen, G. W. Knott *et al.*, Long-term in vivo imaging of

experience-dependent synaptic plasticity in adult cortex. *Nature* **420**, 788-794 (2002).

50. P. Villegas, S. di Santo, R. Burioni, M. A. Muñoz, Time-series thresholding and the definition of avalanche size. *Physical Review E* **100**, 012133 (2019).
51. A. A. Faisal, L. P. J. Selen, D. M. Wolpert, Noise in the nervous system. *Nat Rev Neurosci* **9**, 292-303 (2008).
52. W. Maass, Noise as a Resource for Computation and Learning in Networks of Spiking Neurons. *Proceedings of the IEEE* **102**, 860-880 (2014).
53. L. Gammaitoni, P. Hänggi, P. Jung, F. Marchesoni, Stochastic resonance. *Rev Mod Phys* **70**, 223-287 (1998).
54. S. Kirkpatrick, J. C. D. Gelatt, M. P. Vecchi, Optimization by simulated annealing. *Science* **220**, 671-680 (1983).
55. F. Gassmann, Noise-induced chaos-order transitions. *Physical Review E* **55**, 2215-2221 (1997).
56. K. Matsumoto, I. Tsuda, Noise-induced order. *Journal of Statistical Physics* **31**, 87-106 (1983).
57. N. Ishida, T. I. Shiramatsu, T. Kubota, D. Akita, H. Takahashi, Quantification of information processing capacity in living brain as physical reservoir. *Applied Physics Letters* **122** (in press).